Quaternary-Transformation-Induced Changes at the Heme in Deoxyhemoglobins†

M. R. Ondrias, D. L. Rousseau,* J. A. Shelnutt,‡ and S. R. Simon

ABSTRACT: Quaternary-structure-induced differences in both the high- and low-frequency regions of the resonance Raman spectrum of the heme have been detected in a variety of hemoglobins. These differences may be the result of (1) changes in the amino acid sequence, induced by genetic and chemical modifications, and (2) alterations in the quaternary structure. For samples in solution in low ionic strength buffers, differences in the 1357-cm^{-1} line (an electron-density-sensitive vibrational mode) correlate with differences in the 216-cm^{-1} line (the iron–histidine stretching mode). Thus, changes in the iron–histidine bond and changes in the π-electron density of the porphyrin depend upon a common heme–globin interaction. The quaternary-structure-induced changes in the vibrational modes associated with the heme demonstrate that there is extensive communication between the heme and the globin and impact on models for the energetics of cooperativity. The local interactions of the iron–histidine mode are energetically small and destabilize the deoxy heme in the T structure with respect to the R structure. Therefore, these interactions must be larger in the ligated protein than in the deoxy protein to obtain a negative free energy of cooperativity. Additionally, our data imply that the deprotonation of the proximal histidine does not play a major role in the energetics of cooperativity. On the other hand, models for cooperativity that require conformational changes in the iron–histidine bond or direct interaction between the porphyrin and the protein are qualitatively consistent with the observed variation of heme electronic structure in concert with protein quaternary structure.

Since the earliest observation of the crystallographic dimorphism of deoxy- and oxyhemoglobin (Haurowitz, 1938), the importance of protein quaternary structure for cooperative ligand binding in this protein has been recognized. The nature of the linkage between the large structural rearrangement of the subunits and the formation of the heme–ligand bond, however, has eluded investigators for many years. Only recently have quaternary-structure-induced changes in the hemes (Shelnutt et al., 1979b) and ligand-induced changes in the tertiary structure of the protein subunits been described (Baldwin & Chothia, 1979). The functional significance of many of these changes remains controversial. In the hemes of deoxyhemoglobins we have been able to detect extensive changes which are associated with the quaternary rearrangement of the subunits. These changes may be integral components of the structural perturbations which couple ligand binding to the quaternary conformational transition and which are essential for cooperativity.

The binding of oxygen by hemoglobin (Hb)[1] can be treated successfully by the two-state allosteric approximation in which there are two characteristic quaternary structures of the tetrameric molecule (Shulman et al., 1975). One (the R structure) is the predominant protein conformation when all four ferrous hemes are bound to oxygen, and the other (the T structure) is the predominant conformation of the normal deoxygenated molecule. The cooperative nature of O_2 binding is a result of a $\sim$4 kcal/mol increase in binding energy for oxygen when the globin is in the R structure compared to the binding energy when it is the T structure. Several phenomenologically distinct models have been advanced to explain the origin of this free energy of cooperativity. The models range from those in which the free energy resides in a few localized bonds (Perutz, 1970) to those in which it is distributed throughout the globin with no large fraction of it localized in any one bond (Ogawa & Shulman, 1971; Weber, 1972; Hopfield, 1973). No one model can account for all the experimental data, and thus the molecular basis for cooperativity remains unresolved.

The application of resonance Raman scattering to the problem offers promise for discriminating among the possible mechanisms for cooperativity. Owing to the specificity resulting from resonance enhancement, only vibrational modes of the heme and its axial ligands are observed in Raman scattering spectra of hemoglobin (Spiro & Strekas, 1972) without interference from spectral lines of the surrounding peptides. Moreover, studies may be carried out either under conditions that closely approximate the physiological environment of the active protein or under selectively varied conditions. From Raman studies of model compounds and many heme proteins, the vibrational modes of the porphyrin macrocycle as well as those of the bonds between the central iron atom and its axial ligands have been identified [see, for example, Asher (1981)]. Recent advances in Raman technique have led to the development of Raman difference spectroscopy (RDS) whereby very small differences may be detected between two spectra obtained simultaneously (Laane & Kiefer, 1980; Rousseau, 1981; Shelnutt et al., 1981). This technique allows influences at the heme resulting from structural changes in the globin to be detected reliably. With such a foundation, detailed studies of hemoglobin and associated theoretical analyses should allow both the determination of the amount of energy stored at the heme moiety or in any of the bonds associated with it and the elucidation of the mechanism

† From Bell Laboratories, Murray Hill, New Jersey 07974 (M.R.O., D.L.R., and J.A.S.), and the State University of New York at Stony Brook, Stony Brook, New York (S.R.S.). *Received November 30, 1981.* The work of S.R.S. is supported by National Institutes of Health Grant HL-25780 and American Heart Association Grant 81-810.

‡ Present address: Sandia National Laboratories, Albuquerque, NM 87185.

[1] Abbreviations: HbA, human adult hemoglobin; EPR, electron paramagnetic resonance; NMR, nuclear magnetic resonance; RDS, Raman difference spectroscopy; CD, circular dichroism; NES, *S*-(*N*-ethylsuccinimido)cysteinyl; des-Arg, arginine-141 removed from the COOH terminus of the α chain; IHP, inositol hexaphosphate; DPG, diphosphoglycerate; 2-MeIm, 2-methylimidazole; 1,2-DiMeIm, 1,2-dimethylimidazole; CTAB, cetyltrimethylammonium bromide.

0006-2960/82/0421-3428$01.25/0

through which the globin is signaled that ligation has occurred at each heme site.

The hemes of ligated and deoxyhemoglobins are quite distinct because significant electronic and structural changes accompany the transformation from the 5-coordinate, high-spin, domed heme of deoxyhemoglobnin to the 6-coordinate, spin-coupled, planar heme of oxyhemoglobin. The most useful way to probe the mechanisms of cooperativity is to compare proteins of distinct quaternary structure in the same state of ligation. Such studies may be carried out with chemically modified hemoglobins, mutant hemoglobins, and hemoglobins in the presence of allosteric effectors. There are several reports of resonance Raman scattering investigations in which the effect of quaternary structure on the heme has been studied (Asher, 1981). These include examination of methemoglobins (Scholler & Hoffman, 1979; Asher & Schuster, 1979; Rousseau et al., 1980; E. R. Henry, D. L. Rousseau, S. R. Simon, J. J. Hopfield, and R. M. Noble, unpublished results), various ferrous liganded hemoglobins (Nagai et al., 1980; Tsubaki et al., 1982), and deoxyhemoglobins (Shelnutt et al., 1979b; Nagai et al., 1980; Rousseau et al., 1982). In each case, when adequate sensitivity was available, differences in the frequencies of heme vibrational modes were detected.

Resonance Raman studies of deoxyhemoglobins have led to the detection of systematic quaternary-structure-dependent changes in both the high-frequency modes of the porphyrin macrocycle (Shelnutt et al., 1979b) and the low-frequency line assigned to the iron–histidine stretching mode (Nagai et al., 1980; Nagai & Kitagawa, 1980). The changes in the high-frequency region, in modes demonstrated to be sensitive to π-electron density, led Shelnutt et al. (1979b) to infer that in the R structure the porphyrin moiety has increased π-electron density relative to that of the T structure. In addition, it was proposed that the increased density is a result of a charge-transfer interaction between the heme and near-heme amino acid residues. Phenylalanine CD-1 was cited as having the appropriate stereochemical properties to account for the charge-transfer interaction. On the basis of this interaction, an explanation for cooperativity was outlined. Other peripheral electronic interactions, such as electrostatic and dipole interactions, have also been postulated to result in differential stabilization energies between the R and T states of oxy- and deoxyhemoglobins (Warshel & Weiss, 1981).

Nagai et al. (1980) and Nagai & Kitagawa (1980) reported quaternary-structure-dependent differences in the iron–histidine stretching mode and interpreted their data as evidence for globin-induced strain in the iron–histidine bond. However, in their analysis they concluded that only a very small fraction of the free energy of cooperativity could be stored in this bond. In addition, they proposed that the high-frequency differences reported by Shelnutt et al. (1979b) were a consequence of back-donation from the central iron atom due to variation in the iron–histidine bond length.

EPR results led Peisach et al. (1973) to propose several years ago that control of the physiological properties of heme proteins resulted from the degree of protonation of the proximal histidine. This idea, supported with theoretical calculations by Valentine et al. (1979) and by recent Raman scattering studies of model compounds (Stein et al., 1980), is appealing since it can account for changes induced in the iron–histidine bond by relatively small conformational changes in the protein.

These proposed mechanisms of cooperativity all involve interactions that are localized near the heme, but they differ widely in their qualitative and quantitative assessment of different heme–protein interactions. We have initiated a thorough Raman scattering investigation of deoxyhemoglobins to test these ideas and to determine whether the influence of the protein quaternary structure upon the heme has unique or multiple origins. We have examined the iron–histidine stretching mode and the high-frequency porphyrin modes in a variety of chemically modified and mutant hemoglobins and in model compounds. The proteins probed in solution in low ionic strength buffers display a correlation between the magnitude of the R–T transformation induced differences in the iron–histidine vibrational frequency and the differences in the high-frequency electron density sensitive porphyrin modes. However, the presence of inorganic phosphates affects this correlation. This indicates that there is more than one spectroscopically significant interaction between the porphyrin and the globin. Furthermore the Raman data from model compounds preclude deprotonation of the proximal histidine from playing any significant role in hemoglobin function.

Experimental Procedures

Resonance Raman spectra of solution samples were recorded on a Raman difference spectroscopy (RDS) apparatus previously described (Rousseau, 1981). Modified human hemoglobins (NES-des-Arg-HbA, des-Arg-HbA) were prepared according to the procedure of Kilmartin & Hewitt (1971). Hb Kempsey and carp Hb were isolated and purified by the methods of Bunn et al. (1974) and of Tan et al. (1972), respectively. Stock solutions of Hb were stored in liquid nitrogen or at 4 °C and were routinely passed through Sephadex G-25 columns before being diluted with appropriate buffers to heme concentrations of 300–800 μM. Deoxyhemoglobin samples were prepared by gentle agitation in a nitrogen atmosphere prior to the addition of a slight excess of sodium dithionite. When appropriate, inositol hexaphosphate (IHP) in a buffered solution was added to a final concentration of 2–3 mM.

Model compounds were prepared by adding appropriate amounts of either 2-methylimidazole (2-MeIm) or 1,2-dimethylimidazole (1,2-DiMeIm) and recrystallized CTAB (cetyltrimethylammonium bromide) to buffered solutions of bovine hemin. The samples were reduced by the addition of a small amount of sodium dithionite.

Results

The data reported here were obtained with excitation in the region of the Soret band. As expected, all the deoxyhemoglobins and their derivatives yield qualitatively similar spectra of polarized Raman bands, confirming that their basic heme environments are similar. However, several systematic differences in vibrational frequencies that vary as a function of the protein quaternary and tertiary structures are evident.

In the high-frequency region, it has already been shown that quaternary-structure-dependent differences occur in the des-Arg human hemoglobins (Shelnutt et al., 1979b). As may be seen in Figure 1, differences are also detected in a mutant hemoglobin (Kempsey) and in a hemoglobin of another species (carp). The magnitudes of the differences are sensitive to allosteric effectors such as IHP, and in the des-Arg-Hb system the frequency differences display a dependence upon the presence of inorganic phosphates as well. It is noteworthy that the large quaternary-structure-dependent differences seen in the 1567-cm^{-1} mode of human hemoglobins are absent in the difference spectrum of carp hemoglobin. Differences have also been observed between human deoxyhemoglobin and its isolated chains or sperm whale myoglobin. These frequency differences are listed in Table I. For entries where there is only a dash, either measurements were not made or the data were of insufficient quality to make a reliable determination of the difference. The entries enclosed in parentheses are from

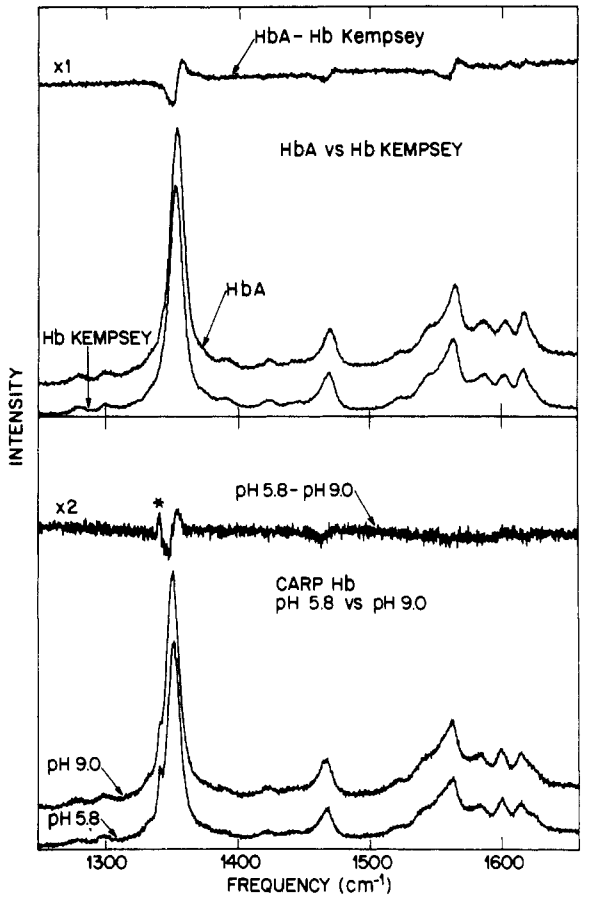

FIGURE 1: High-frequency Raman spectra of deoxyhemoglobins. (Upper panel) HbA vs. Hb Kempsey; (lower panel) carp Hb at pH 5.8 and 9.0. The difference spectrum generated from each pair of simultaneously obtained spectra is displayed above the two separate spectra. For these and spectra in subsequent figures the conditions were 4579-Å excitation at 100–300 mW, 100–200-μm slits (4–12 scans accumulated at 12–24 cm^{-1}/min), heme concentration of 300–800 μM in 50–100 mM Bis-Tris or Tris buffered solutions. The asterisk denotes features caused by laser fluorescence.

comparisons in which one of the samples showed signs of denaturation at the completion of the data acquisition. In each comparison, if a significant oxygen-binding-affinity difference exists between the two human hemoglobins, the high-frequency Raman lines are shifted to lower frequency when the protein is in the higher affinity structure. This is especially evident for the 1357-cm^{-1} line for which this systematic variation in frequency extends to myoglobin and carp hemoglobin. This mode has been shown to be the most reliable indicator of π-electron density in a number of model hemes (Spiro & Strekas, 1974); its frequency is sensitive to quaternary structure in methemoglobins as well (Rousseau et al., 1980).

Systematic changes (Table I) were also seen in the low-frequency (50–500 cm^{-1}) region of the spectrum for the same series of hemoglobins. In Figure 2 we present the comparison between the NES-des-Arg modification and native deoxyhemoglobin A. When the intensities of the ~300-cm^{-1} line are normalized, the more "T-like" structures have the following properties in contrast to the more "R-like" structures: (1) The diffuse scattering is more intense in the low-frequency region (0–300 cm^{-1}), and there is evidence of some weak structure below 150 cm^{-1}. (2) The line in the 160–170-cm^{-1} region has higher intensity and lower frequency. (3) The iron–histidine stretching mode (222 cm^{-1} in NES-des-Arg-HbA) is shifted to lower frequency, has lower intensity, and has a more asymmetric shape. (4) The lines at 340, 361, and 430 cm^{-1}

Table I: Raman Frequency Differences Comparing High-Affinity to Low-Affinity Globins[a]

	differences at varying modes (cm^{-1})					
	160	216	1357	1471	1567	1605
NES-des-Arg vs. HbA	8	6	−1.3	−1.8	−2.2	−1.5
NES-des-Arg ± IHP	3	3	−0.7	−0.9	−1.1	−0.6
des-Arg (pH 9) vs. HbA	8	5	−1.5	–	–	–
des-Arg (pH 9) vs. des-Arg (pH 7)	3	2	−0.5	–	–	–
des-Arg (pH 7) vs. NES-des-Arg (pH 7)*	–	2	−1.1	–	–	–
des-Arg (pH 7) vs. (pH 8.6)*	–	2	−0.8	−1.0	−1.2	−0.7
des-His-Tyr vs. HbA	–	–	(−0.4)	(−0.9)	(−0.7)	(−0.7)
Kempsey (pH 6.5) vs. HbA	1	2	−0.3	−0.6	−0.5	–
Kempsey (pH 9) vs. HbA	2	5	−0.9	−1.4	−1.7	−1.2
Kempsey (pH 6.5) ± IHP	–	2	−0.3	−0.5	−0.6	–
α chains vs. HbA	5	3	−0.6	–	–	–
β_4 tetramers vs. HbA	6	6	−1.4	–	–	–
β_4 tetramers vs. α chains	–	3	−1.0	–	–	–
$\alpha_1\beta_1$ dimers vs. HbA	–	–	(−0.6)	(−0.5)	(−1.1)	(−0.8)
Mb (sperm whale) vs. HbA*	–	3	−1.3	0	−4.2	0
carp Hb (pH 9) vs. carp Hb (pH 6)	–	3	−0.6	−1.3	0	–

[a] All samples were in less than 100 mM Bis or Bis-Tris buffers except those denoted by an asterisk which were in 200 mM phosphate.

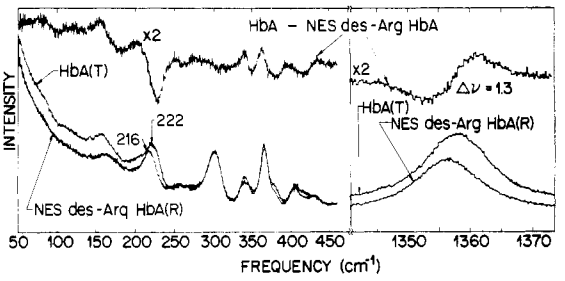

FIGURE 2: Comparison of HbA (T state) and NES-des-Arg-HbA (R state) at room temperature in low-frequency and "oxidation-state marker" regions. The features displayed in the difference spectra of these regions are qualitatively representative of all comparisons made between human hemoglobins having different oxygen affinities. For this and all comparisons of low-frequency spectra, the raw spectra are normalized so that the intensities of the ~300-cm^{-1} band (which is invariant upon R–T conversion) are equal before the difference spectrum is generated.

increase in intensity, and the features at 355, 380, and 420 cm^{-1} decrease in intensity.

A comparison of HbA and Hb Kempsey at pH 9 (shown in Figure 3) reveals qualitatively similar changes. Although these differences were also seen between HbA and Hb Kempsey at pH 6.5, they were significantly smaller (see Table I). Comparison of carp Hb at low and high pH shows the first three characteristic differences listed above but not the fourth; i.e., changes in features from 340 to 420 cm^{-1} were much less pronounced. α chains and β_4 tetramers give spectra similar to those of the R-state hemoglobins, but as may be seen in Table I, there are significant differences between the two isolated chains.

The properties of the iron–histidine system were examined by studying the spectra of ferroprotoporphyrin IX complexed

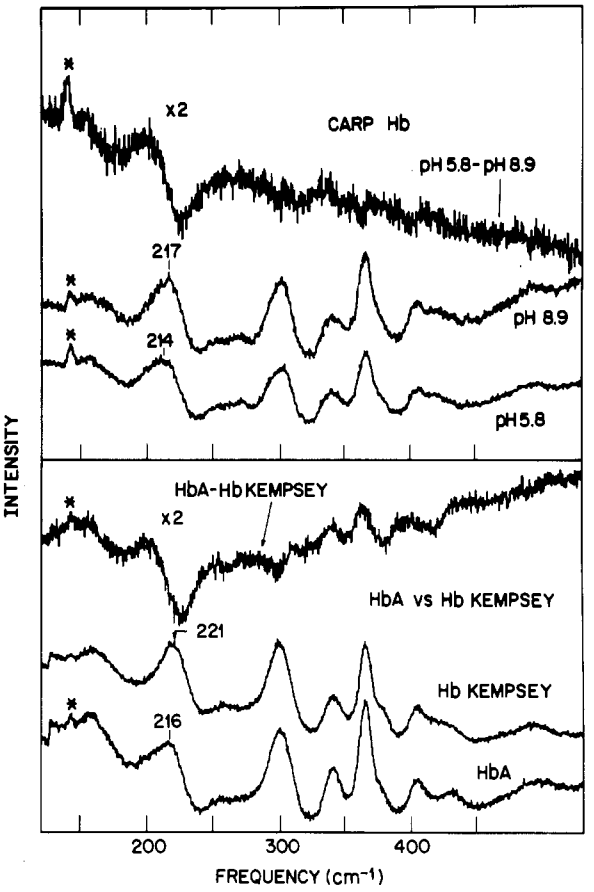

FIGURE 3: Comparison of the low-frequency regions of carp Hb at pH 5.8 (T state) and pH 8.9 (R state) (upper panel) and HbA vs. Hb Kempsey (R state) (lower panel). Conditions were the same as those described in Figure 1.

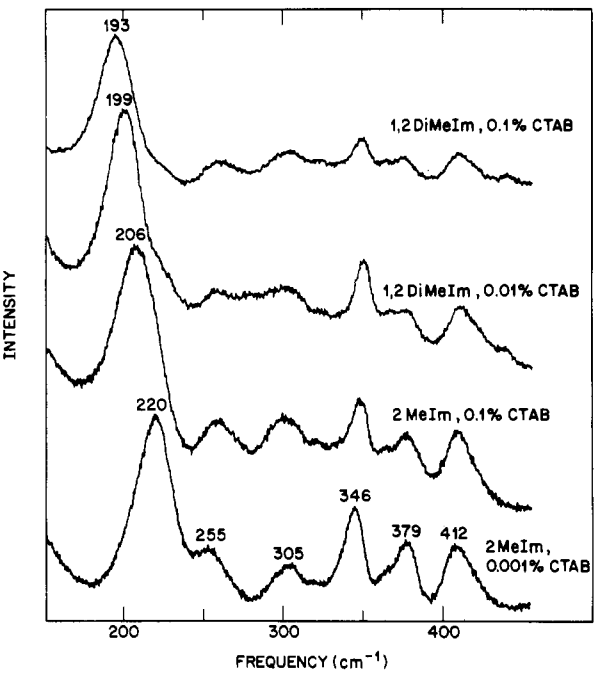

FIGURE 4: Spectra of the low-frequency regions of protoporphyrin IX complexes with 1,2-dimethylimidazole (1,2-DiMeIm) and 2-methylimidazole (2-MeIm) in varying concentrations of cetyltrimethylammonium bromide (CTAB). Note that the addition of detergent affects the properties of the iron–histidine stretching mode even in the 1,2-DiMeIm model compound which has no labile N-1 proton. Conditions are the same as those described in Figure 1.

with 2-methylimidazole and 1,2-dimethylimidazole. These 5-coordinate, out-of-plane (0.4-Å) complexes serve as model compounds for deoxyhemoglobins (Jameson et al., 1978). The iron–ligand bond of these complexes is sensitive to the presence of detergents (Hori & Kitagawa, 1980). Shifts in the iron–imidazole stretching frequency could be induced in aqueous solutions of both the 2-methylimidazole and the 1,2-dimethylimidazole complexes by increasing the concentration of the detergent CTAB from 0.001% to 0.1% (see Figure 4). Large changes (up to 3 cm^{-1}) in the line at 1357 cm^{-1} were also detected as a function of the CTAB concentration in these complexes (Figure 5). It is interesting to note that the 1357-cm^{-1} line and the iron–histidine stretching mode both shift to *lower* frequencies upon increasing CTAB concentrations in Fe(II) protoporphyrin XI–2-MeIm solutions or upon replacement of 2-MeIm with 1,2-diMeIm; on the other hand, the 1357-cm^{-1} line shifts to *higher* frequencies, while the frequency of the iron–histidine stretch declines, upon transition of the protein quaternary structure from R to T in deoxyhemoglobins. As the CTAB concentration increases, the 1,2-dimethylimidazole model compound displays a large shift ($\sim$6 cm^{-1}) in the frequency of the iron–histidine stretching mode but no corresponding change in frequency in the 1357-cm^{-1} region. Table II contrasts the spectral changes induced in the model compounds with those exhibited by the proteins.

Table II: Frequency Differences in the Iron–Histidine Stretching Frequency Region (200–230 cm^{-1}) and the Electron-Density Marker Line (1357 cm^{-1}) for Model Compounds[a]

	frequency differences at	
	200–230	1357
HbA–NES-des-Arg-HbA	−6	+1.3
2-MeIm ± CTAB	−14	−1.7
1,2-DiMeIm–2-MeIm	−13	−3.3
1,2-DiMeIm ± CTAB	−6	0

[a] Note the change in the relative directions of the differences in the model compounds as compared to the HbA–NES-des-Arg-HbA differences.

Discussion

The Raman spectra of porphyrins and heme proteins are well characterized and have been shown to be rich in information concerning the nuances of the heme structure. Specific Raman modes are sensitive to π-electron density in the porphyrin macrocycle (Spiro & Strekas, 1974), certain Raman modes are sensitive to the size of the porphyrin core (Spaulding et al., 1975), and axial ligand stretching modes have been identified. Comparing Raman spectra of two very similar materials permits sensitive detection of differences. The utility of using Raman difference spectroscopy to probe subtle protein–heme interactions has been demonstrated (Shelnutt et al., 1979a). A careful examination of the relationship between systematic changes detected in the porphyrin macrocycle of hemoglobin that are a function of the quaternary structure is a crucial step toward identifying and understanding the role that the globin plays in controlling the reactivity of the active site.

High-Frequency Region. Electron density in the porphyrin π orbitals, spin equilibrium in the heme iron, and the size of the "core" between the pyrrole nitrogens have all been shown to influence several lines in the 1200–1700-cm^{-1} region of the Raman spectrum. In particular the modes above 1400 cm^{-1} are sensitive to the iron spin state and to the size of the porphyrin core. This sensitivity to core size is probably a result of porphyrin distortion at the meso carbons upon heme ex-

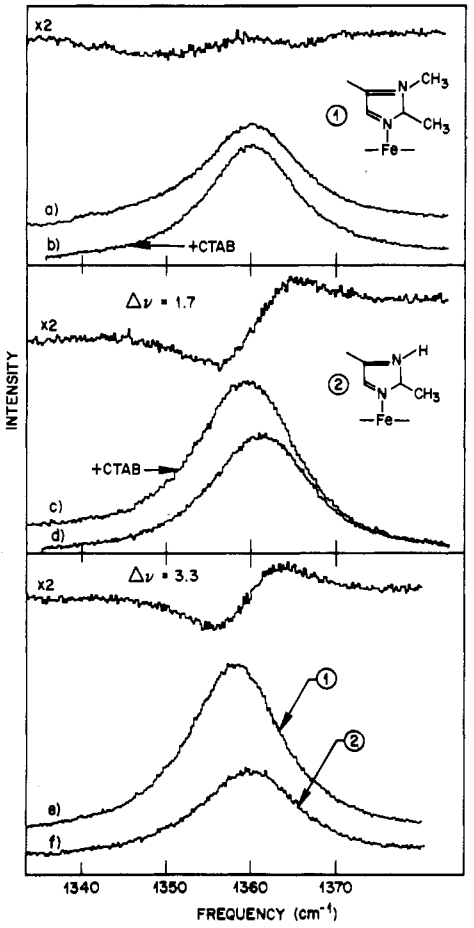

FIGURE 5: Changes in the oxidation-state marker band in protoporphyrin IX complexes as a function of axial ligand and CTAB concentration. (Upper panel) Comparison of 1,2-dimethylimidazole complexes in 0.01% CTAB (a) and 0.1% CTAB (b). (Middle panel) Comparison of 2-methylimidazole complexes in 0.1% CTAB (c) and 0.001% CTAB (d). (Lower panel) Comparison of 1,2-dimethylimidazole complexes (e) and 2-methylimidazole complexes (f) both in 0.1% CTAB. Samples are the same as those from which the low-frequency spectra in Figure 6 were obtained. Conditions were the same as those described in Figure 1.

pansion (Warshel, 1977; Teraoka & Kitagawa, 1980). The sensitivity to π-electron density is especially clear in the polarized mode at 1357 cm^{-1}, as it is independent of changes in the core size. The behavior of this mode upon variation in the electron density of the antibonding π^* orbitals of the porphyrin macrocycle has been extensively studied in metalloporphyrins and heme proteins (Spiro et al., 1979). It systematically changes frequency with variation of the π-donating properties of axial ligands and predictably changes frequency with oxidation state and formation of porphyrin anions. A comparison of calculated π-electron density in osmium porphyrins (Antipas et al., 1980) with Raman frequencies of iron mesoporphyrins with the same axial ligands (Spiro & Burke, 1976) supports the correlation between π-electron density and frequency of the polarized line at 1357 cm^{-1}.

Recently, Shelnutt (1981) found shifts in the high-frequency Raman lines of Cu uroporphyrin that result from π–π charge-transfer complex formation with derivatives of phenanthroline and other aromatic heterocycles. A correlation between the shifts in a group of lines, including the oxidation state marker line at 1379 cm^{-1}, and the acceptor abilities of the phenanthroline derivatives was found. An exception to this correlation is the hindered derivatives that will not lie flat on the porphyrin ring. However, the group of phenanthrolines for which the correlation was evident did include a derivative that has sterically hindered lone pairs on the ring nitrogens. Therefore, π–π donor–acceptor interaction between the aromatic ring systems was conclusively shown. These results further support the identification of a group of high-frequency π-electron density marker lines of the porphyrin for conditions under which other factors, such as spin state and core size, are unchanged.

The data presented in this paper and elsewhere (Shelnutt et al., 1979b) show that a general trend exists in comparisons between the spectra of high-affinity and low-affinity globins in the 1200–1700-cm^{-1} region. Among the various human hemoglobins, all of the lines respond in a concerted manner, shifting to lower frequency upon conversion to the high-affinity forms. However, in the comparison of deoxymyoglobin to deoxyhemoglobin, we detected no difference in the 1471-cm^{-1} line, although large changes were still detected in other modes. Similarly, in a comparison of carp hemoglobin at high and low pH, there is no change in the 1567-cm^{-1} line. In all cases differences are observed in the 1357-cm^{-1} line. The variation in the response of the high-frequency modes is not especially surprising since most of these modes are sensitive to several influences such as spin-state variations, core size, and electron density. Furthermore, many have normal mode contributions from the vinyl side chains and other peripheral substituents (Abe et al., 1978; M. R. Ondrias, D. L. Rousseau, K. M. Smith, and G. N. LaMar, unpublished results; T. Kitagawa, K. Nagai, K. M. Smith, and G. N. LaMar, unpublished results). On the contrary, the 1357-cm^{-1} line has no contribution from peripheral substituents and is insensitive to porphyrin-core size. The absence of one or more peripheral interactions may account for the differences between the extensive concerted changes in the spectra of various human hemoglobins and the more selective changes in the spectra of carp hemoglobin and myoglobin.

The range of values observed for the changes in the 1357-cm^{-1} line results from tertiary structural differences in the heme pocket. These may arise from inherent differences between the globins being compared, or they may be induced by changes in the quaternary structure. When the frequency differences for the same hemoglobin in the presence or absence of an allosteric effector are examined, these two contributions can be separated. Several such comparisons indicate that the contribution from the quaternary structure alone is about 0.7 $\pm$ 0.2 cm^{-1}. In those comparisons in which there are large differences, the remaining contributions probably result from inherent tertiary structural differences between the two hemoglobins. The variations in the results for Hb Kempsey as a function of pH will be discussed in the next section.

Low-Frequency Region. We have also detected systematic quaternary-structure-dependent differences in the low-frequency region. As in the high-frequency region, the pattern of these changes is the same in all comparisons among human hemoglobins. This is apparent upon examination of the shape of the difference spectra in Figure 2 (des-Arg-HbA vs. HbA comparison) and in Figure 3 (Hb Kempsey vs. HbA comparison). Unfortunately, the normal mode assignments of the low-frequency modes are not as yet sufficiently detailed to allow determination of the structural significance of the systematic variations in the 300–500-cm^{-1} region. In a preliminary assignment by Kitagawa & Nagai (1982), the lines at 300 and 345 cm^{-1} were attributed to symmetric breathing modes of the entire porphyrin macrocycle coupled with motions involving peripheral substituents. Extensive isotopic studies are needed to confirm these assignments. It is interesting to note that the quaternary-structure differences are significantly

reduced in the carp difference spectra (Figure 3) as compared to those obtained with the human hemoglobins. As in the high-frequency region, this may result from differences in one or more peripheral interactions.

The mode at 216 cm^{-1} in HbA displays large differences in all comparisons among globins with different affinities. This mode is of particular interest because it has been assigned as the iron–histidine stretching frequency from isotopic substitution studies of the iron in model compounds, hemoglobin, and myoglobin and in deuteration studies of the coordinated imidazole. The changes we detect in this mode in the chemically modified, mutant, and carp hemoglobins indicate a quaternary-structure-induced change in the iron–histidine bond in which the frequency of this mode is lower in the T structure than in the R structure. The behavior of this bond is pivotal to an understanding of the molecular mechanisms of oxygen binding because the bond is trans to the oxygen binding site. Moreover, proposed mechanisms of cooperativity that rely upon deprotonation of the proximal histidine or steric interactions due to histidine tilt require localization of a significant fraction of the free energy of cooperativity in this iron–histidine bonding interaction. Just as in the high-frequency region, examination of the large body of data allows a crude separation of the contribution of the change in quaternary structure from that resulting from inherent tertiary structural differences. This analysis yields a quaternary-structure-dependent difference of 3 ± 1 cm^{-1} in the peak frequency of this mode.

Changes in the low-frequency region of valency hybrid hemoglobins were previously reported by Nagai & Kitagawa (1980). They concluded that the asymmetric shape observed for HbA is a consequence of chain distinguishability, the α chain having a peak near 203 cm^{-1} and the β chain having a peak near 218 cm^{-1}. A recent study of the cobalt/iron hybrids (Ondrias et al., 1982) has confirmed a large R–T splitting in the α chains and a very small splitting in the β chains. Corresponding differences were found in the high-frequency region as well. Since none of the data reported here was collected from hybrid hemoglobins, our results necessarily represent averages of the α and β chains.

It is noteworthy that we have detected frequency differences between Hb Kempsey and HbA. Kincaid et al. (1979) detected no differences in the low-frequency region when they made this same comparison. However, their experiments were conducted at pH 7.2. We found that at pH 6.5 the differences between HbA and Hb Kempsey are very small (see Table I). Only by raising the pH of the Hb Kempsey to 9 were we able to detect the large differences shown in Figures 1 and 3. Preliminary CD measurements and NMR measurements (Nagai et al., 1982) of the N-1 proton suggest that, at the low pH, Hb Kempsey is predominantly in the T state rather than in the R state. This could account for the very small differences detected in our low pH experiments as well as those reported by Kincaid et al. (1979). The implications of these results for the properties of Hb Kempsey will be discussed in a separate report.

The origin of the mode at 160 cm^{-1} has not yet been assigned. However, it displays changes in frequency that parallel those of the iron–histidine stretching mode and appears to undergo complementary changes in intensity. The possibility that the 160- and the 216-cm^{-1} modes correspond to two radically different conformations of the iron–histidine bond remains to be explored.

Heme–Protein Interactions. Since both the iron–histidine bond strength and the porphyrin electron density influence the electron density and distribution at the heme iron, it may be

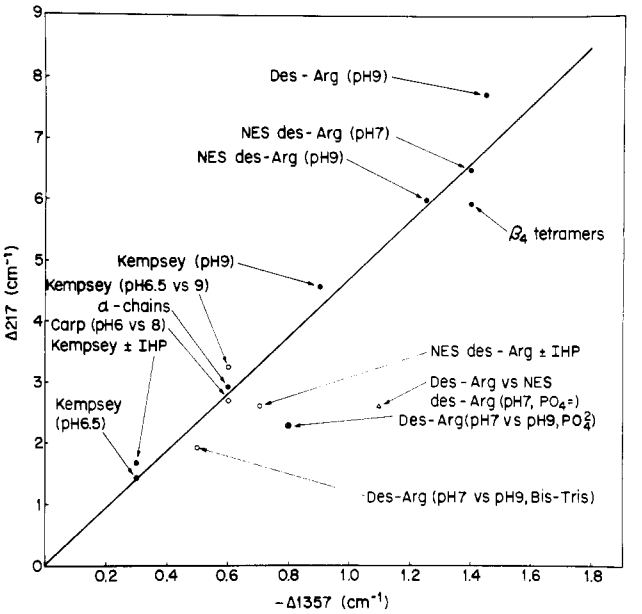

FIGURE 6: Correlation between differences in the 1357-cm^{-1} band and the Fe–His stretching frequency for a variety of hemoglobins. Note that the changes on the abscissa go in the negative direction. All values are for the comparison of the indicated hemoglobin with HbA unless otherwise noted. Comparisons are grouped as follows: (○) involves only quaternary transformation; (●) involves both quaternary and inherent tertiary differences; (△) obtained in a phosphate buffer.

anticipated that changes in the two regions are coupled. Any changes in either iron–histidine bonding or the porphyrin electron density could be expected to give rise to a change in the electronic environment of the iron and hence be transmitted to the other. Furthermore, since modulation of the porphyrin π-electron density is sensitive to the degree of iron d_π-to-porphyrin π back-bonding, it would be expected that changes in the π bonding of the iron to the axial ligand would couple more strongly to the porphyrin π system than would a change in the σ bonding of the ligand. Thus, iron–histidine and porphyrin electron-density responses to protein quaternary structure need not be orthogonal to each other. From such considerations, Nagai & Kitagawa (1980) and Perutz (1980) concluded that globin-induced changes in the iron–histidine bond can give rise to electron-density changes in the porphyrin macrocycle. We have found that there is a correlation among frequency shifts of the electron-density marker line and iron–histidine stretching mode. On the other hand, this correlation is altered for some modified hemoglobins in the presence of inorganic phosphates. Below we discuss the details of these results and some of their implications.

The change detected in the iron–histidine stretching frequency is plotted against the change in frequency of the 1357-cm^{-1} line in Figure 6 for a series of globins. Although there is some scatter in the plot, it is quite apparent that there is indeed a linear correlation between the data in these two regions. It is noteworthy that in the carp protein these two modes are the *only* ones in which we have detected significant differences. We infer from the correlated changes under low ionic strength conditions that however many interactions between the heme and the protein may be contributing to the frequencies of these lines, these interactions are concerted. Furthermore, the correlation applies to comparisons in which only the quaternary structure is changed as well as those in which the inherent tertiary structure is varied by chemical or genetic modification. The magnitude of the contribution of the quaternary-structure change to the Raman difference

spectrum appears to be independent of the inherent tertiary environment of the hemoglobin. This is true for the carp, des-Arg-HbA, NES-des-Arg-HbA, and Hb Kempsey systems (see Figure 6), suggesting that the effects of changing the quaternary structure upon the local heme environment, as reflected by the behavior of these two modes, are equivalent for these diverse globins.

The correlated linear response of the 1357-cm^{-1} line and the iron–histidine stretching mode suggests a common origin for the frequency differences detected in these two modes. As proposed by Nagai & Kitagawa (1980) and by Perutz (1980), the differences in the porphyrin skeletal mode could result from changes in back-donation due to alterations of the iron–histidine bond. However, the inverse is also possible, namely, that variations in the heme electron density due to changes in the porphyrin environment could alter the iron–histidine electronic structure. Or finally, changes in both of these modes could be linked only through some third interaction. It is difficult to distinguish among these possibilities and to assign causality to related changes detected at the heme since the energies involved in heme-related interactions such as globin tension, steric hindrance, histidine deprotonation, charge-transfer interactions, and electrostatic interactions remain undetermined.

To study further the relationship between these two modes, we have examined the correlated responses in the two spectral regions under a variety of conditions. We have found for the des-Arg-Hb system that the relationship between the frequency of the iron–histidine mode and the electron-density marker line is different in the presence of inorganic phosphates than it is in low ionic strength buffers. Effects on the properties of modified hemoglobins caused by the presence of inorganic phosphate are not unexpected. Baldwin (1975) reported that those modified hemoglobins with only moderate increases in oxygen affinity and reductions in cooperativity, such as des-Arg-Hb, and hemoglobin reacted with NEM alone, show progressive increases in the Hill constant, n, and the allosteric equilibrium constant, L, upon replacement of dilute buffers by inorganic phosphate, DPG, and IHP in sequence. NES-des-Arg-hemoglobin, on the other hand, shows no cooperativity and has a value of L of less than 1 even in the presence of DPG. It is therefore not surprising that we failed to detect any effects of inorganic phosphate on this derivative.

Transient resonance Raman measurements of the deoxy spectrum following photolysis of CO are also consistent with coupled changes in these two regions of the spectrum. Friedman (J. M. Friedman, unpublished results) recently examined the time dependence of both the iron–histidine stretching mode and the electron-density marker line (ν_4). He found that the time dependence of the changes in frequency of the two modes was correlated from 10 ns to several microseconds. Furthermore, the frequency differences in these modes, compared to the corresponding modes in deoxy-HbA, lie on the same correlation curve (Figure 6) as reported here.

As a comparison to the hemoglobin results, we have monitored the behavior of the iron–histidine mode and the 1357-cm^{-1} electron-density marker line in model compounds as their environment is changed. Under conditions in which frequency of the 220-cm^{-1} line decreases, the line at 1357 cm^{-1} also decreases, or remains unchanged. As seen in Table II, this is the opposite of the behavior that we have observed in the proteins, supplying additional evidence that a unique chemical linkage in the behavior of these two lines does not exist. However, the linear correlation between the 1357-cm^{-1} line and the iron–histidine stretching mode suggests that the changes in both modes result from a single interaction in the protein.

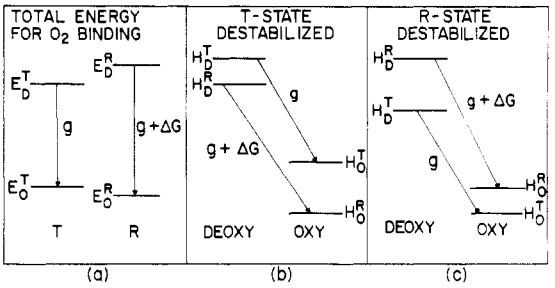

FIGURE 7: Energy level diagrams for cooperative interactions. (a) Total energy, E, for binding O_2 in the T state and in the R state; (b) heme–protein interactions when the T state is destabilized; (c) heme–protein interactions when the R state is destabilized.

Energetics of Cooperative Interactions. Determination of the energetics of cooperativity from interactions that are detected at the heme requires expressions for the total energy, E, for each structure of the protein in the liganded and unliganded states. To obtain these, we assume a two-state allosteric model so that intermediate steps in the oxygenation process need not be considered. Thus for T structure deoxyhemoglobin (D) we obtain (following Shelnutt, 1980)

$$E_D^T = P_D^T + H_D^T \quad (1)$$

Similarly for T structure oxyhemoglobin (O)

$$E_O^T = P_O^T + H_O^T + B_O^T \quad (2)$$

Equivalent expressions may be written for the R structure. P is the protein–protein interaction energy, H is the heme–protein interaction energy, and B is the hemoglobin–exogenous ligand interaction energy. The significance of each of these terms will be discussed in detail below. Within the two-state model (Shulman et al., 1975), we may define the free energy of cooperativity, ΔG, as the difference between binding O_2 in the R state and in the T state ($\Delta G = -RT \ln c$, where c, the allosteric model parameter, is the ratio of the dissociation constants for ligands from the R state and from the T state). Referring to Figure 7, ΔG may be written as

$$\Delta G = (E_O^R - E_D^R) - (E_O^T - E_D^T) \quad (3)$$

From eq 3 we then obtain three terms for the free energy of cooperativity.

$$\Delta G = P + B + H \quad (4)$$

$$P = (P_O^R - P_O^T) - (P_D^R - P_D^T) \quad (5)$$

$$B = (B_O^R - B_O^T) \quad (6)$$

$$H = (H_O^R - H_O^T) - (H_D^R - H_D^T) \quad (7)$$

The first term, P (eq 5), describes the protein–protein interactions and includes all the quaternary-structure changes within the protein (but not in the heme cages) and at the subunit interfaces. It should be noted that within the distributed-energy model a large number of small changes in the protein–protein interactions are included in P. The second term, B (eq 6), contains any direct interaction between the exogenous ligand and the globin. Finally, the last term, H (eq 7), describes the interactions between the heme and the amino acids which can interact directly with it. A second parameter in the allosteric two-state model, F ($F = -RT \ln L$, where L is the ratio of the concentrations of the unliganded T and R structures) may be defined as

$$F = E_D^T - E_D^R = (H_D^T - H_D^R) - (P_D^R - P_D^T) \quad (8)$$

Within the framework of these arguments, it must be stressed that the localized interactions detected at the heme are an expression of the constraints imposed by the entire protein assuming its most energetically favorable conformation. Any destabilization evident in the heme–protein interactions of T-state deoxy-HbA does not imply an overall increase in energy ($E_D^T \gg E_D^R$). In fact, minimization of F dictates that the protein exists in the T state. Similarly, the combined effects of H, P, and B must be considered in assessing the equilibrium configuration of oxygenated hemoglobins. The importance of each type of interaction to the energetics of cooperativity stems not from its absolute magnitude (which determines the thermodynamics of overall protein confrontation) but rather from the relative change in each upon conversion between R and T states. Thus, we are, in effect, looking for a rather small change in the energy of a very large system. The problem can be made more tractable by examining the possibility and ramifications of finding ΔG in the more localized interactions B and H.

There have been measurements of the properties of the exogenous ligand to the iron bond in several systems including liganded methemoglobins (Asher, 1981), oxyhemoglobin (Nagai et al., 1980a), and (carbon monoxy)hemoglobin (Tsubaki et al., 1982). In all cases no R–T differences were detected in the iron-to-ligand bond. Thus, B (eq 6) makes no contribution to ΔG. Several models for cooperativity postulate that a large fraction of ΔG is localized in interactions involving the heme. The implications of these models may be explored by assuming that the contribution to ΔG from the ligation-dependent changes in protein–protein interactions (eq 5) is zero. Under this assumption, ΔG would be localized in the heme–protein interactions (eq 7). This places no restrictions, however, on the contributions to F. Simple diagrams shown in Figure 7 may be used to illustrate the possible energy levels of those bonds in which the free energy of cooperativity could be localized. It is interesting to examine the systematic energetics under these restricted conditions. Consider the case (Figure 7b) in which heme–protein interactions destabilize the T structure. Then, for the free energy of cooperativity to be nonvanishing (negative ΔG), the destabilization of the T structure must be *larger* in the oxygenated form of the protein than in the deoxygenated form. On the other hand, if the interactions were to destabilize the R structure (Figure 7c), this destabilization would have to be larger in deoxyhemoglobin in order for a negative ΔG to result. However, it must be kept in mind that some of the data presented here and elsewhere argue for the existence of multiple heme–protein interactions. Thus, there may be several contributions to ΔG. To the extent that these apparently concerted interactions can be separated into axial (imidazole–iron–ligand) and peripheral (heme–ligand–heme pocket) components, it is possible to consider the implications of the present body of spectroscopic data for various models of hemoglobin function.

Models for Cooperativity. On the basis of perturbations detected at the heme, some models for hemoglobin cooperativity have cited specific molecular interactions that destabilize the deoxyhemoglobin T structure. For example, several proposals estimate the energy stored in the iron–histidine bond from the changes in the Raman spectra of deoxyhemoglobins (Nagai et al., 1980; Kincaid et al., 1979). These investigators have assumed either that steric strain introduced distortion in a single "diatomic" iron–histidine bond potential or that electronic effects (deprotonation of the imidazole N-1 position) created different "diatomic" potentials in the R and T states of deoxyhemoglobin. Regardless of the assumptions made about the bond potential, the lower frequency of the T structure iron–histidine mode relative to that of the R structure indicates that the T structure is destabilized. Quantification of the destabilization energy is model dependent and ranges from 0.01 to 1.0 kcal/mol per heme, the larger value being derived from Morse potential (D_e = 10 kcal) calculations using the average of the contributions from the α and β chains. The destabilization has ramifications for both F and ΔG which are independent of the details of the interactions assumed to give rise to iron–histidine bond-energy differences. The destabilization must be balanced by an even larger protein–protein interaction and/or other heme–protein interactions to account for the net T-state *stabilization* in deoxyhemoglobin ($F = \sim 8$ kcal). In the same vein, if these interactions make an energetically significant contribution to ΔG, they must have a larger effect in liganded hemoglobin. Unfortunately, the frequency of the iron–histidine mode has not been located in the liganded heme. However, we may consider the implications of having a large contribution from the iron–histidine energetics for the properties of oxyhemoglobin. In the R structure, which has a stronger iron–histidine bond, there would be an enhanced imidazole–iron interaction as compared to the T structure. Presumably this change in electronic structure would modulate the strength of the Fe–O_2 bond and would be detected in an R–T comparison of that bond. However, as cited above, several measurements of the iron–exogenous ligand bond properties have been made, and in all cases thus far reported no significant R–T differences in the properties of such bonds have been found.

Several other independent considerations argue specifically against deprotonation of the proximal imidazole as being a causative agent in hemoglobin cooperativity. Analysis of the model-compound data presented here suggests that variations in the degree of deprotonation is not the dominant mechanism which gives rise to the R–T differences in the iron–histidine mode of deoxyhemoglobin. First, as shown in Figure 4, we have detected a substantial change in the iron–histidine stretching mode with increased concentrations of CTAB in solutions of 1,2-dimethylimidazole–protoporphyrin IX in which the N-1 position of the imidazole has a methyl group rather than a proton. Thus deprotonation is not the only vehicle for inducing shifts in the model compounds. Second, the changes that are induced by alteration of the solvent environment and axial ligand structure result in a relationship between the frequency shifts in the 220-cm^{-1} line and the 1357-cm^{-1} line which is the reverse of that seen in the R–T transition in hemoglobin. These frequency changes in the 220-cm^{-1} line were cited by Stein et al. (1980) as evidence that deprotonation had occurred in these model compounds, and these investigators suggested that this process was operative in hemoglobin as well. However, if deprotonation were the origin of the 220-cm^{-1} line changes in hemoglobin, then a very large compensatory interaction at the heme periphery would have to occur to account for the direction of the characteristic shift in the 1357-cm^{-1} line seen in all hemoglobins examined. As further evidence that variation in deprotonation is not the origin of the changes in the iron–histidine region, the NMR resonance of the N-1 proton is detected in *both* the R and the T states (G. N. LaMar, private communication). The small ($\sim$15 ppm) separation is consistent with small changes in iron–histidine bond strain, and by comparison with NMR and Raman data obtained from other heme proteins, it is not consistent with deprotonation.

Electronic interaction models cite the differences detected in the electron-density marker line between deoxyhemoglobin and ligated hemoglobin as evidence for a large change in porphyrin electron density upon ligation. In both the deoxy and the ligated states differential electronic interactions between the heme and the globin, caused by charge-transfer, electrostatic, or dipolar forces, are postulated to result in energetic distinctions between the R and T structures. Furthermore, the depletion of porphyrin π-electron density upon ligation (or oxidation) could be expected to produce distinct interactions in the ligated and unligated forms of HbA. Changes in the electron-density marker line have been detected as a function of quaternary structure in ligated hemoglobins (D. L. Rousseau, S.-L. Tan, M. R. Ondrias, S. Ogawa, and R. M. Noble, unpublished results), in methemoglobins (Rousseau et al., 1980), and in the ferrous deoxyhemoglobins, reported here. In marked contrast to the behavior of the deoxy proteins in both the ligated and the methemoglobins, the mode appears at a *lower* frequency in the T state by 0.2–0.8 cm^{-1}. An additional probe of local heme–protein interactions in ligated hemoglobins is the detection of heme spectra immediately after ligand dissociation by photolysis and before significant tertiary or quaternary rearrangements can occur. Friedman et al. (1982) found that differences between photolyzed and fully relaxed hemoglobins were qualitatively similar but significantly larger than those seen in R–T comparisons of deoxyhemoglobins. This qualitative difference in behavior between the ligated and methemoglobins compared to the just-photolyzed and relaxed deoxyhemoglobins makes a quantitative assessment of the energy associated with the changes in the local electronic environment of the heme difficult. However, even though an understanding of the details is lacking, the electronic models as a class are compatible with the observation of a change in the heme electronic environment as a function of quaternary structure for deoxy as well as ligated hemoglobins. Further work must be done to assess whether this apparent change in electronic properties results directly from a protein–heme interaction or is a signature of other interactions, such as a change in the histidine orientation.

Conclusions

Several points emerge from this study. (1) For all quaternary-structure comparisons in human deoxyhemoglobins, a systematic variation in several modes was detected. These include changes in the iron–histidine mode as well as changes in porphyrin ring modes having contributions from peripheral constituents. (2) In low ionic strength phosphate-free buffers there is a correlation between the frequencies of the iron–histidine mode (200–230 cm^{-1}) and the electron-density marker line (1355–1360 cm^{-1}). This correlation is evident in carp hemoglobin and in chemically and genetically modified human hemoglobins as well, suggesting that in the absence of other perturbations a single heme–globin interaction is responsible for the quaternary-structure sensitivity of these modes. (3) The correlation between these modes is altered for some of the chemically modified hemoglobins by the presence of inorganic phosphates. This indicates that these modes may be affected independently by other protein–heme interactions.

These data bear on cooperativity and mechanisms of hemoglobin function in the following ways: (1) The quaternary-structure-induced changes in vibrational modes associated with the heme demonstrate that there is extensive communication between the heme and the globin. (2) Model-compound data reported here as well as NMR data reported elsewhere indicate that deprotonation of the proximal histidine does not play a major role in the energetics of cooperativity. (3) The iron–histidine mode changes resulting from the quaternary-structure transition are small and destabilize the T structure in deoxyhemoglobin. For the energy of this bond to significantly contribute to cooperativity, the changes must be much larger in the ligated protein. However, no evidence for large changes in this bond has been found in the ligated protein. (4) It cannot yet be assessed whether the systematic changes seen in the porphyrin vibrational modes result from energetically significant heme–protein interactions or whether they are indicative of energy storage in protein–protein interactions remote from the heme.

Acknowledgments

We thank N.-T. Yu and G. N. LaMar for communicating results to us prior to publication. We thank J. J. Hopfield, J. M. Friedman, and T. Kitagawa for helpful discussions. We have benefited from a critical reading of the manuscript by S. Neuhauser. The carp hemoglobin samples were generously supplied by R. W. Noble and the hemoglobin Kempsey by H. F. Bunn.

References

Abe, M., Kitagawa, T., & Kyogoku, Y. (1978) *J. Chem. Phys. 69*, 4526–4534.

Antipas, A., Buchler, J. W., Gouterman, M., & Smith, P. D. (1980) *J. Am. Chem. Soc. 102*, 198–207.

Asher, S. A. (1981) *Methods Enzymol.* (in press).

Asher, S. A., & Schuster, T. M. (1979) *Biochemistry 18*, 5377–5387.

Baldwin, J. M. (1975) *Prog. Biophys. Mol. Biol. 29*, 225–320.

Baldwin, J., & Chothia, C. (1979) *J. Mol. Biol. 129*, 175–220.

Bunn, H. F., Wohl, R. C., Bradley, T. B., Cooley, M., & Gibson, Q. H. (1974) *J. Biol. Chem. 249*, 7402–7409.

Friedman, J. M., Stepnoski, R. A., Stavola, M., Ondrias, M. R., & Cone, R. (1982) *Biochemistry 21*, 2022–2028.

Haurowitz, F. (1938) *Z. Physiol. Chem. 254*, 266–276.

Hopfield, J. J. (1973) *J. Mol. Biol. 77*, 207–222.

Hori, H., & Kitagawa, T. (1980) *J. Am. Chem. Soc. 102*, 3608–3613.

Jameson, G. B., Molinaro, F. S., Ibers, J. A., Collman, J. P., Brauman, J. I., Rose, E., & Suslick, K. S. (1978) *J. Am. Chem. Soc. 100*, 6769.

Kilmartin, J. V., & Hewitt, J. A. (1971) *Cold Spring Harbor Symp. Quant. Biol. 36*, 311–314.

Kincaid, J., Stein, P., & Spiro, T. G. (1979) *Proc. Natl. Acad. Sci. U.S.A. 76*, 549–552.

Kitagawa, T., & Nagai, K. (1982) in *Interaction Between Iron and Proteins in Oxygen and Electron Transport* (Ho, C., Ed.) pp 217–222, Elsevier/North-Holland, New York.

Laane, J., & Kiefer, W. (1980) *J. Chem. Phys. 72*, 5305–5311.

Nagai, K., & Kitagawa, T. (1980) *Proc. Natl. Acad. Sci. U.S.A. 77*, 2033–2037.

Nagai, K., Kitagawa, T., & Morimoto, H. (1980) *J. Mol. Biol. 136*, 271–289.

Nagai, K., La Mar, G. N., Jue, T., & Bunn, H. F. (1982) *Biochemistry 21*, 842–847.

Ogawa, S., & Shulman, R. G. (1972) *J. Mol. Biol. 70*, 315–336.

Ondrias, M. R., Rousseau, D. L., Kitagawa, T., Ikeda-Saito, M., Inubushi, T., & Yonetani, T. (1982) *J. Biol. Chem.* (in press).

Peisach, J., Blumberg, W. E., & Adler, A. (1973) *Ann. N.Y. Acad. Sci. 206*, 310–326.

Perutz, M. E. (1970) *Nature (London) 228*, 726–734.

Perutz, M. E. (1980) *Proc. R. Soc. London, Ser. B B208*, 135–162.

Rousseau, D. L. (1981) *J. Raman Spectrosc. 10*, 94–99.
Rousseau, D. L., Shelnutt, J. A., Henry, E. R., & Simon, S. R. (1980) *Nature (London) 285*, 49–51.
Rousseau, D. L., Shelnutt, J. A., Ondrias, M. R., Friedman, J. M., Henry, E. R., & Simon, S. R. (1982) in *Interaction Between Iron and Proteins in Oxygen and Electron Transport* (Ho, C., Ed.) pp 223–229, Elsevier/North-Holland, New York.
Scholler, D. M., & Hoffman, B. M. (1979) *J. Am. Chem. Soc. 101*, 1655–1662.
Shelnutt, J. A. (1980) *C.R.—Int. Conf. Spectrosc. Raman: 7th*, 516–519.
Shelnutt, J. A. (1981) *J. Am. Chem. Soc. 103*, 4275–4277.
Shelnutt, J. A., Rousseau, D. L., Dethmers, J. K., & Margoliash, E. (1979a) *Proc. Natl. Acad. Sci. U.S.A. 76*, 3865–3869.
Shelnutt, J. A., Rousseau, D. L., Friedman, J. M., & Simon, S. R. (1979b) *Proc. Natl. Acad. Sci. U.S.A. 76*, 4409–4413.
Shelnutt, J. A., Rousseau, D. L., Dethmers, J. K., & Margoliash, E. (1981) *Biochemistry 20*, 6485.
Shulman, R. G., Hopfield, J. J., & Ogawa, S. (1975) *Q. Rev. Biophys. 8*, 325–420.
Spaulding, L. D., Chang, C. C., Yu, N.-T., & Felton, R. H. (1975) *J. Am. Chem. Soc. 97*, 2517–2525.
Spiro, T. G., & Strekas, T. C. (1972) *Proc. Natl. Acad. Sci. U.S.A. 69*, 2622–2626.
Spiro, T. G., & Strekas, T. C. (1974) *J. Am. Chem. Soc. 96*, 338–345.
Spiro, T. G., & Burke, J. M. (1976) *J. Am. Chem. Soc. 98*, 5482–5489.
Spiro, T. G., Stong, J. D., & Stein, P. (1979) *J. Am. Chem. Soc. 101*, 2648–2655.
Stein, P., Mitchell, M., & Spiro, T. G. (1980) *J. Am. Chem. Soc. 102*, 7795–7797.
Tan, A. L., DeYoung, A., & Noble, R. W. (1972) *J. Biol. Chem. 247*, 2493–2498.
Teraoka, J., & Kitagawa, T. (1980) *J. Phys. Chem. 84*, 1928–1935.
Tsubaki, M., Srivastava, R. B., & Yu, N.-T. (1982) *Biochemistry 21*, 1132–1140.
Valentine, J. S., Sheridan, R. P., Allen, L. C., & Kahn, P. C. (1979) *Proc. Natl. Acad. Sci. U.S.A. 76*, 1009–1013.
Warshel, A. (1977) *Annu. Rev. Biophys. Bioeng. 6*, 273.
Warshel, A., & Weiss, R. M. (1981) *J. Am. Chem. Soc. 103*, 446–451.
Weber, G. (1972) *Biochemistry 11*, 864–878.

Role of Meizothrombin and Meizothrombin-(des F1) in the Conversion of Prothrombin to Thrombin by the *Echis carinatus* Venom Coagulant†

Moo-Jhong Rhee, Sam Morris, and David P. Kosow*

ABSTRACT: The venom of the saw scaled viper, *Echis carinatus*, contains a protein capable of converting prothrombin to an active enzyme. This prothrombin activator (ECV-P) has been purified 40-fold by affinity chromatography on wheat germ agglutinin–Sepharose 4B followed by ion-exchange chromatography on DEAE-Sephacel. ECV-P was homogeneous as assessed by dodecyl sulfate–polyacrylamide gel electrophoresis. Sialic acid, neutral sugars, and hexosamines were present at 4.2, 7.2, and 5.8 wt %, respectively. Amino acid analysis of reduced and carboxymethylated ECV-P revealed an unusually high cysteine content of 9 mol %. ECV-P is inhibited by chelators such as ethylenediaminetetraacetic acid and *o*-phenanthroline but is active after treatment with Chelex. However, atomic absorption studies revealed that neither Ca, Co, Cr, Cu, Fe, Mn, Ni, nor Zn ion is present at more than 0.01 mol/mol of active protein after Chelex treatment. Gel electrophoretic studies in the presence and absence of inhibitors were performed to determine the initial products of the reaction of ECV-P with human prothrombin. In the presence of diisopropyl fluorophosphate, or benzamidine, the major product is meizothrombin-(des F1). However, when dansylarginine *N*,*N*-(3-ethyl-1,5-pentanediyl)amide (DAPA) was utilized as an inhibitor of any thrombin-like enzymes which are formed by ECV-P, the initial product was meizothrombin; meizothrombin-(des F1) appeared as a second product. By removal of ECV-P after the production of meizothrombin and addition of additional prothrombin, it was demonstrated that meizothrombin can convert prothrombin to prethrombin-1, prethrombin-2, and thrombin. Similarly, meizothrombin-(des F1), produced from the reaction of ECV-P with prethrombin-1, can also convert prothrombin to these products. These results demonstrate that unlike thrombin, meizothrombin and meizothrombin-(des F1) can convert prothrombin to an active enzyme.

The activation of prothrombin is the last step of the series of zymogen to enzyme conversions which are involved in the coagulation cascade. During normal blood clotting, this step is catalyzed by the coagulation enzyme factor Xa, with Ca^{2+}, phospholipid, and factor Va acting as cofactors (Suttie & Jackson, 1977). Prothrombin can also be converted to an active enzyme by specific proteases obtained from the venoms of the Taipan snake, *O. scutellatus* (Denson et al., 1971; Owen & Jackson, 1973), the boomslang, *D. typus* (Mackay et al., 1969; Guillin et al., 1978), the tiger snake, *N. scutellatus scutellatus* (Jobin & Esnouf, 1966), and the saw scaled viper, *Echis carinatus* (Schieck et al., 1972; Franza et al., 1975; Kornalik & Blomback, 1975; Morita et al., 1976). In the course of our studies on prothrombin activation, we became interested in using the venom coagulant enzyme of *E. carinatus* (ECV-P)[1] as a model system for the study of prothrombin

† From the Plasma Derivatives Laboratory, American Red Cross Blood Services Laboratories, Bethesda, Maryland 20014. *Received August 12, 1981.* Contribution No. 447. This work was supported in part by Research Grant HL19282 and Biomedical Support Grant 5 S07 RR05737 from the National Institutes of Health.

0006-2960/82/0421-3437$01.25/0